# Characterization and optimization of tin particle mitigation and EUV conversion efficiency in a laser produced plasma EUV light source

Tatsuya Yanagida*, Hitoshi Nagano[a], Yasunori Wada, Takayuki Yabu, Shinji Nagai, Georg Soumagne, Tsukasa Hori, Kouji Kakizaki[a], Akira Sumitani, Junichi Fujimoto[b], Hakaru Mizoguchi[b] and Akira Endo[c]
EUVA, 3-25-1 Shinomiya Hiratsuka Kanagawa 254-8555, Japan;
[a]KOMATSU Ltd., 3-25-1 Shinomiya Hiratsuka Kanagawa 254-8555, Japan;
[b]Gigaphoton Inc., 400 Yokokura shinden, Oyama, Tochigi, 323-8558, Japan;
[c]Forschungzentrum Dresden, Germany

## ABSTRACT

A laser produced plasma (LPP) extreme ultraviolet (EUV) light source of 13.5 nm has been developed for next generation lithography. Sn plasma is an efficient generator of 13.5 nm EUV light. On the other hand, deposition of Sn particles which strongly affects EUV collector mirror lifetime is a critical issue for long-term stable operation of the high-power EUV light source. In this paper we describe about the optimization of tin debris mitigation with a compact EUV generation system. We observe almost all of Sn fragments generated after a pre-pulse irradiation are vaporized by a main $CO_2$ pulse laser with a droplet of 20 μm in diameter. An EUV conversion efficiency (CE) of 3.4% at a maximum is obtained for the 20 μm droplet. These results indicate the debris mitigation can be achieved without degradation of the high EUV CE.

**Keywords:** EUV light source, Laser-Produced Plasma, Sn droplet, Debris, EUV conversion efficiency, laser induced fluorescence, Shadowgraph

## 1. INTRODUCTION

An extreme ultraviolet (EUV) light source of 13.5 nm has been developed for next generation lithography. A promising method to generate in particular the required high output power of over 250 W is a laser produced plasma (LPP) with a Sn droplet target and a pulsed $CO_2$ laser, because a Sn plasma can produce a high conversion efficiency at 13.5 nm.

On the other hand, deposition of Sn particles which strongly affects EUV mirror lifetime is a critical issue for long-term stable operation of the high-power EUV light source. Only about 1 nm Sn deposited on the EUV collector mirror, i.e. only several atomic layers, reduces the mirror reflectivity by 10%, which is considered as the mirror lifetime specification.

Sn particles, also called “debris”, consist of fragments, neutral atoms and energetic plasma ions. We previously reported Sn debris characteristics from $CO_2$ laser driven plasmas using bulk Sn-plate targets and Mo/Si multilayer mirror samples[1,2]. We observed very thin and uniform Sn layers of nano/sub-nano size debris particles on Mo/Si multilayer mirror samples. The layer deposition rate at 120 mm from the plasma is about 30 nm per million shots. In addition, we have demonstrated a fivefold reduction in deposition rate of Sn layer due to a reduction of the ion number at the sample mirror by applying a static magnetic field of 1 T[3,4,5] because the Sn ions are converged and ejected on the direction of the magnetic field. In this configuration, a high ionization degree of the Sn particles enhances the guiding. An effective way to obtain high ionization and therefore high mitigation performance is to supply smaller Sn droplets with a diameter of 10 to 20 μm. However, there is a possible risk that the EUV conversion efficiency (CE) decreases for smaller droplets because of an insufficient Sn supply to generate the plasma . In order to maintain a high EUV CE, precise control of laser irradiation conditions is required.

*tatsuya_yanagida@komatsu.co.jp; http://www.euva.or.jp

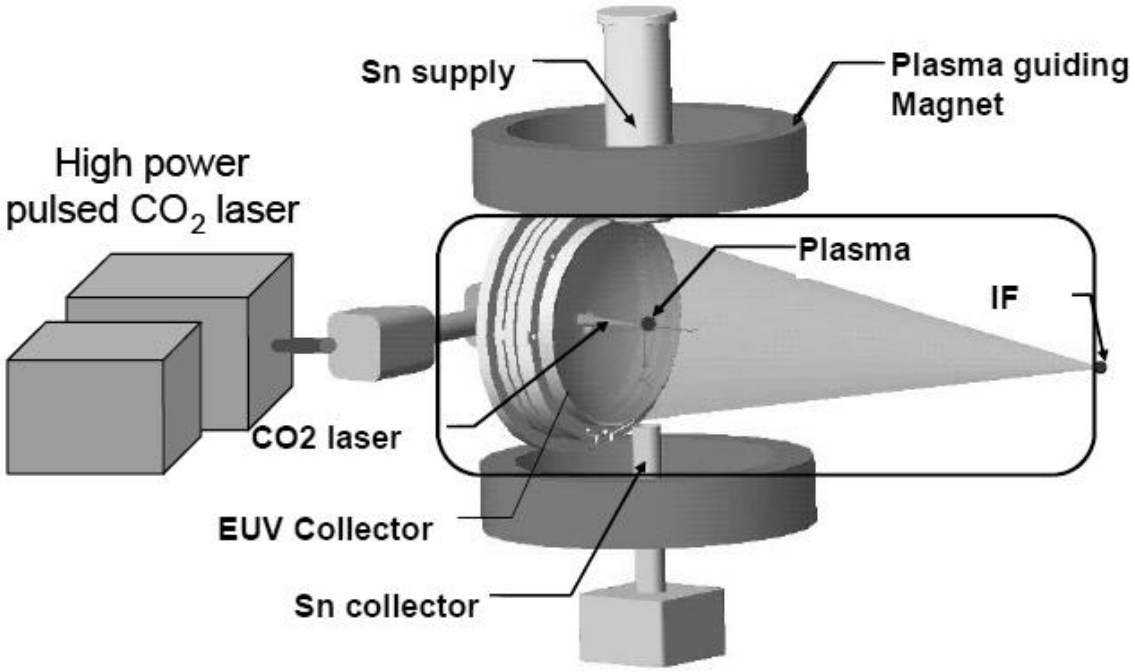


Figure 1. Schematic diagram of the developing LPP EUV light source system

A compact EUV generation system is employed for basic investigation of EUV light generation and Sn particles mitigation. In this paper, we describe the characteristics of the Sn debris from the 20 μm droplet and a mitigation performance after the optimization of the pre-pulse laser and the main-pulse laser conditions. The EUV CEs for the small droplets are also reported.

## 2. DEBRIS MITIGATION SCHEME FOR LPP EUV SOURCE

Figure 1 shows the schematic diagram of the developing LPP EUV light source system. The LPP EUV system mainly consists of a Sn droplet generator, a pre-pulse laser for a preliminary conditioning of the Sn target, a short-pulsed high-energy $CO_2$ laser for driving the EUV plasma, and the EUV vacuum chamber with a EUV collector mirror and a magnet. Liquid micro-droplets generated by the Sn droplet generator are synchronously irradiated by the pre-pulse laser and the $CO_2$ laser with an appropriate timing and other irradiation conditions. Then the generated EUV light is collected at the intermediate focus (IF) by the EUV collector mirror. The system operates at a pulse repetition rate of 100kHz. A key feature of the system is a Sn debris mitigation using the magnetic field. It is possible to collect the Sn ions effectively, and prevent the degradation of the EUV collector mirror[6]. The Sn debris are roughly classified into three particles; Sn fragments, neutral atoms and ions[7]. Figure 2 represents the velocity distribution for each particle. As shown in the figure the ions have the fastest speed, and second fastest particle is the neutrals.

In our LPP system, the debris are reduced to practical level by the following method,

- The Sn droplets are supplied with minimum size required for the EUV generation.
- The Sn fragments generated after the pre-pulse laser irradiation are vaporized and ionized by the main $CO_2$ pulse laser.
- The Sn ions are trapped by the magnetic field and collected.
- Residual Sn neutrals which may be deposited on the collector mirror are cleaned

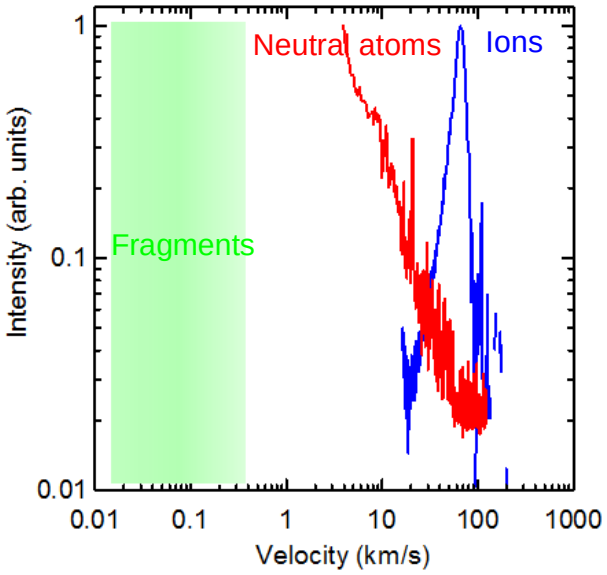


Figure 2. Velocity distribution of the Sn particles from a laser produced plasma

We investigate the fragments, generated from the droplet target irradiated by the pre-pulse laser, vaporization by the $CO_2$ pulse laser irradiation. We also observed the behavior of the neutral atoms from a planar target irradiated by the pre-pulse laser with a laser induced fluorescence (LIF) technique. The effect of magnetic field for the neutral atoms is studied.

As noted before, supplying the droplet with smaller diameter is desirable for reducing the total amount of the Sn debris. However, the EUV CE may degrade because of a lack of a Sn fuel. So far, EUV CE over 3% has been reported for the droplet diameter of over 30 μm[8]. The optimization of the EUV CE for the droplet of 20 μm in diameter is presented.

## 3. EXPERIMENTAL SETUP

Figure 3 shows the experimental setup for basic investigation of EUV light generation and Sn particles mitigation. Figure 4 shows the outlook of the setup. This system simulates the same conditions, for example pulse width and pulse energy of a $CO_2$ laser, tin droplet size and magnetic field, as the high-power EUV light source we develop except for the pulse repetition rate. Because of the compactness of the system it is easy to measure and optimize many irradiation parameters. The EUV system mainly consists of a short-pulsed high-energy $CO_2$ laser, a pre-pulse laser, a tin droplet generator and a EUV vacuum chamber with a solenoid magnet. The droplet generator can supply a droplet with a diameter of 10 μm at a minimum. The system operates at a frequency of 10Hz. The vacuum chamber is evacuated by a turbo molecular pump. As previously described, Sn debris are generally classified into fragments, neutral atoms and ions. Sn fragments are measured by a shadowgraph method with a short-pulsed back illuminator and a CCD camera with a high-resolution telescope. Figure 5 shows a shadowgraph image of Sn droplet with a diameter of 20 μm. In order to investigate a behavior of Sn neutral atoms under a high-magnetic field, Sn atoms from laser plasma with a planar target are measured by LIF method. Sn atoms are excited by a 3rd harmonics of narrow-band Ti:sapphire laser which is tuned at the transition of $5p^2\ ^3P_0 - 6s\ ^3P^o_1$ (286.3 nm). The fluorescence from the transition of $5p^2\ ^3P_2 - 6s\ ^3P^o_1$ (317.5 nm) is observed with an image intensified CCD (ICCD) camera through a band-pass filter[9]. The energy level diagram of Sn atom is shown in Figure 6. A Two-dimensional atom distributions are obtained with a thin line-profiled laser beam probed from a direction perpendicular to the Sn target surface.

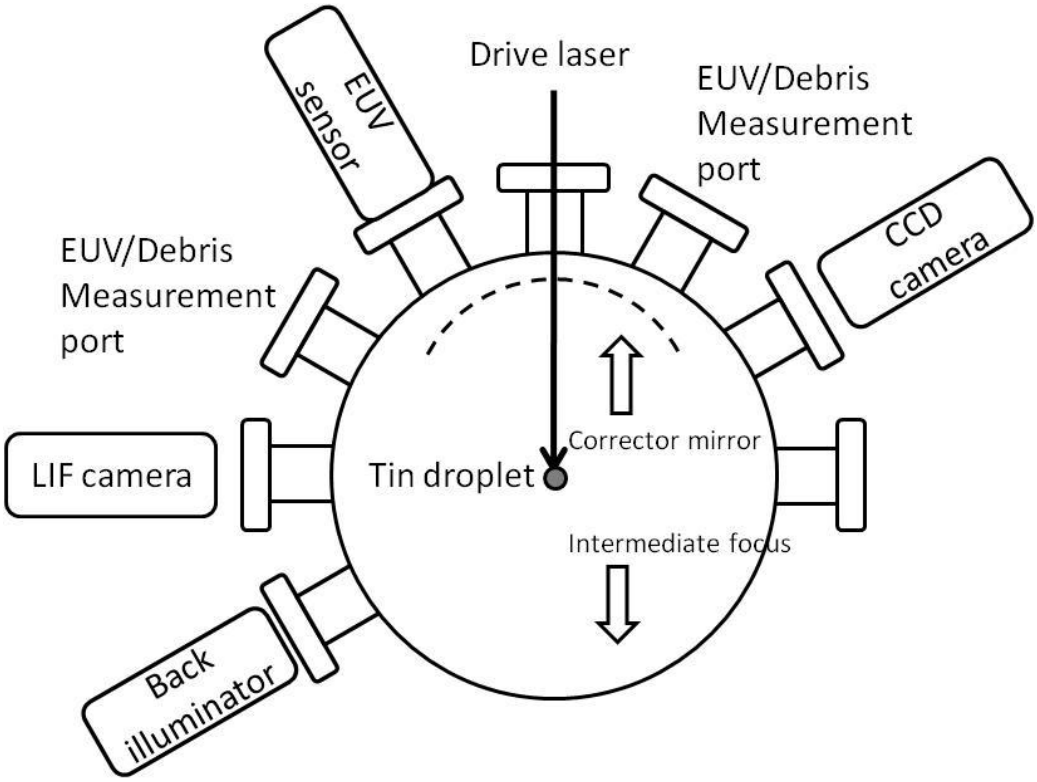


Figure 3. Experimental setup for basic investigation of EUV light generation and tin particles mitigation

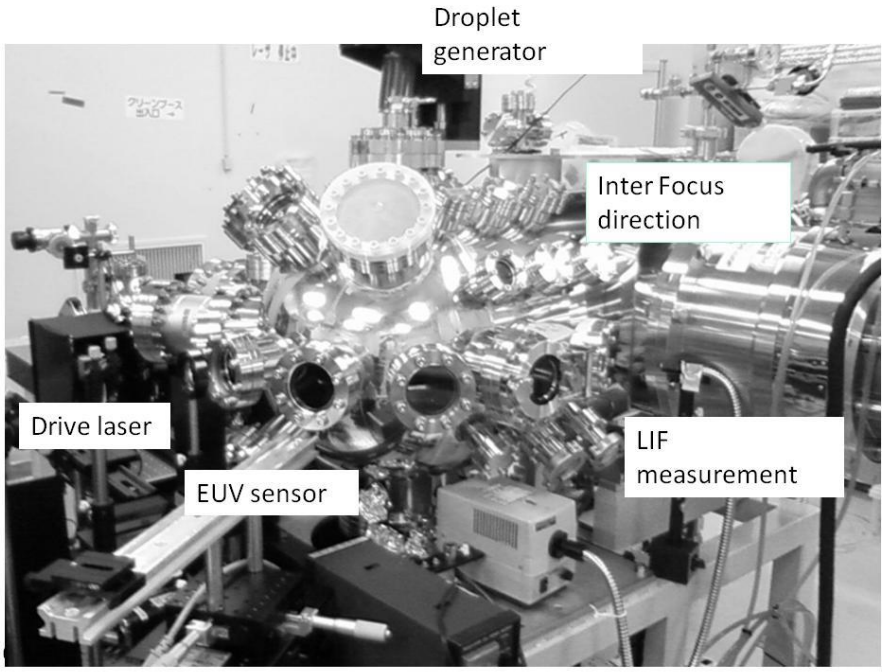


Figure 4. Outlook of the experimental setup

Other debris measurement tools, for example a faraday cup and a witness plate, are installed into the chamber.
A 13.5 nm EUV output is measured by a EUV sensor which consists of a Mo/Si mirror, a Zr filter and a Si detector at 30 degree from the laser incident direction. A EUV CE integrated over 2 π steradian into a 2% in-band is calculated by the EUV sensor output assuming the isotropic EUV radiation.

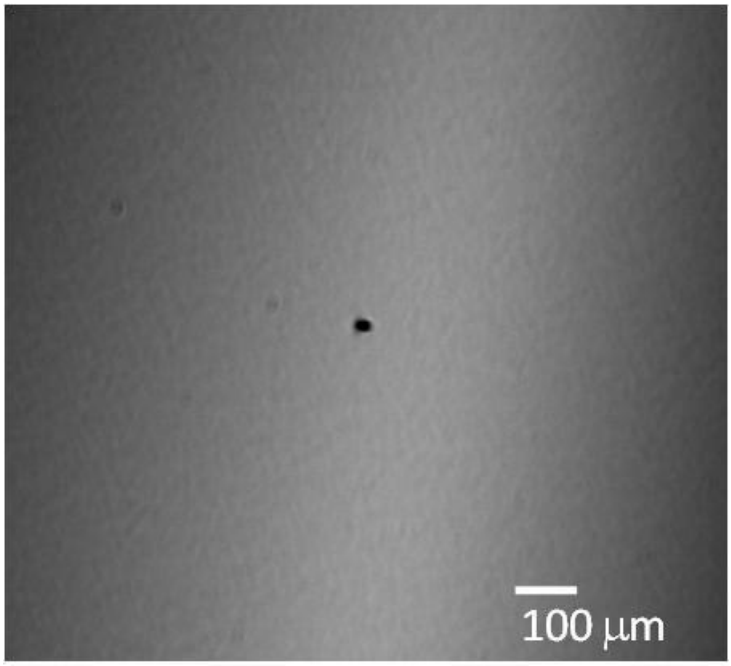


Figure 5. Shadowgraph image of 20 μm diameter Sn droplet

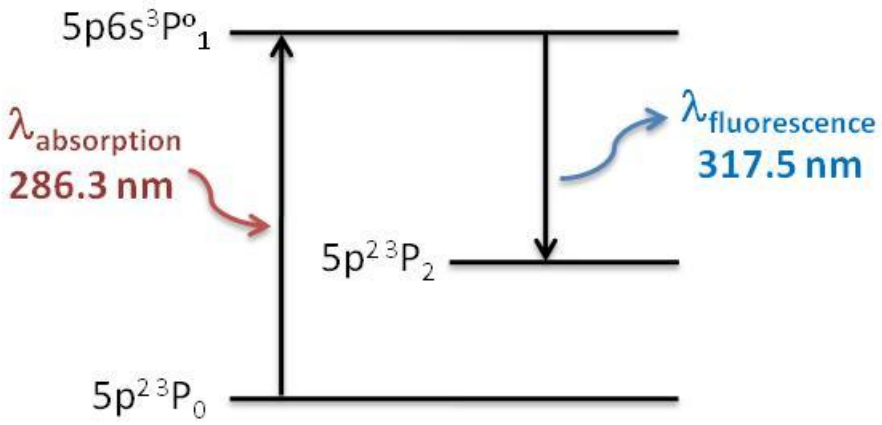


Figure 6. Energy level of Sn atom

# 4. RESULTS AND DISCUSSION

## 4.1 Fragment imaging

Sn fragments are generated after the pre-pulse irradiation. The Sn fragment is a majority of Sn debris. The diameter of the fragment reaches a few micrometers at a maximum. Figure 7 shows the shadowgraphs of the fragments after the pre-pulse laser irradiation for the droplet with 20 μm in diameter. The pre-pulse laser is irradiated onto the droplet from the left hand side of the image. After laser irradiation, the droplet is moved to the opposite side while expanding larger diameter. Figure 7a shows the images after the pre-pulse laser irradiation without the main $CO_2$ laser pulse irradiation. Figure 7b shows the images with the main $CO_2$ laser pulse. The center image is captured during the main pulse irradiation. The right-hand image is captured just after the EUV plasma emission. In this case, the fragments are vanished from the shadowgraph image. We believe almost all of the fragments are at least vaporized. Figure 7 is the ideal case optimized the laser irradiation conditions. On the other hand, figure 8 shows an example of a wrong laser irradiation condition. The right-hand shadowgraph image of figure 8b is obtained after the main laser pulse irradiation. Quite a few fragments still remain without vaporization. As a consequence of the experiment, it is found that fragments generated after the pre-pulse irradiation can be vaporized, then probably ionized, by reducing the droplet size below 20 μm and optimizing the laser irradiation parameters.

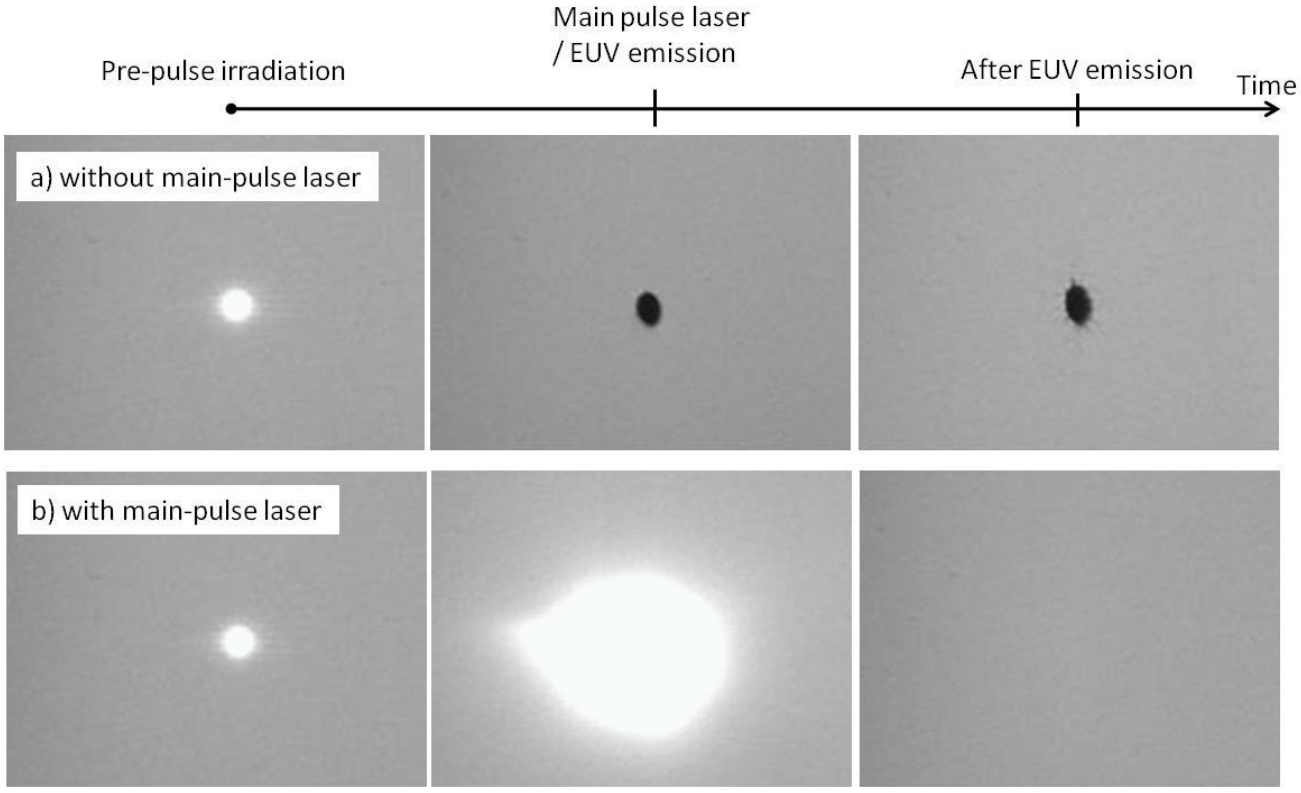


Figure 7. Shadowgraph images of the Sn fragments I (a proper condition)

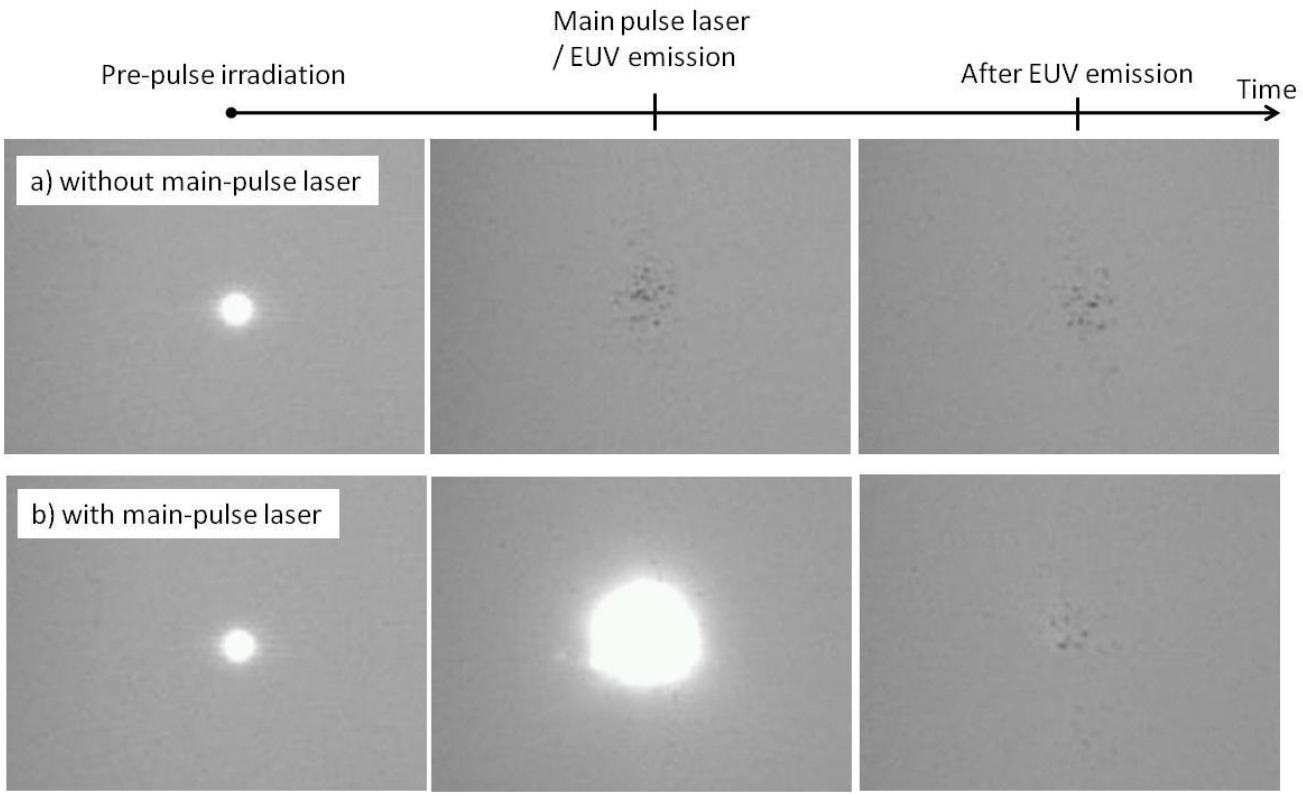


Figure 8. Shadowgraph images of the Sn fragments II (a wrong condition)

\

### 4.2 LIF measurement of Sn neutrals from a planar target in a strong magnetic field

Figure 9 shows the LIF two-dimensional contour images of the neutral distributions generated from a planar Sn target irradiated by the pre-pulse laser. These images are observed after 1 μs from the pre-pulse laser irradiation. The left figure represents the distribution without the magnetic field. The Sn atoms expand isotropic. In contrast, when the laser is irradiated in a strong magnetic field, the right figure, the Sn atoms strongly converge on the direction of the magnetic field. This indicates that the magnetic field helps guiding the Sn particles of not only the charged particle but also the neutral atom.

### 4.3 EUV CE measurement

Figure 10 shows the EUV CE as a function of the droplet diameter. The pre-pulse is a key parameter for a higher EUV CE. The EUV CE reached to 3.4% for the 20 μm droplet by optimizing the pre-pulse laser conditions. Figure 11 depicts the EUV clean pulse energy for the 20 μm droplet as a function of the pulse energy of the $CO_2$ laser under the optimum pre-pulse condition. The maximum EUV-CE is observed for the $CO_2$ pulse energy of 134 mJ at a maximum. It is clear that the EUV CE doesn't saturate in the $CO_2$ pulse energy range. The equivalent clean EUV power which is calculated with the condition of our developing system with the pulse repletion rate of 100kHz also represents in figure 11. The maximum EUV clean power of 100 W is expected for the system condition.

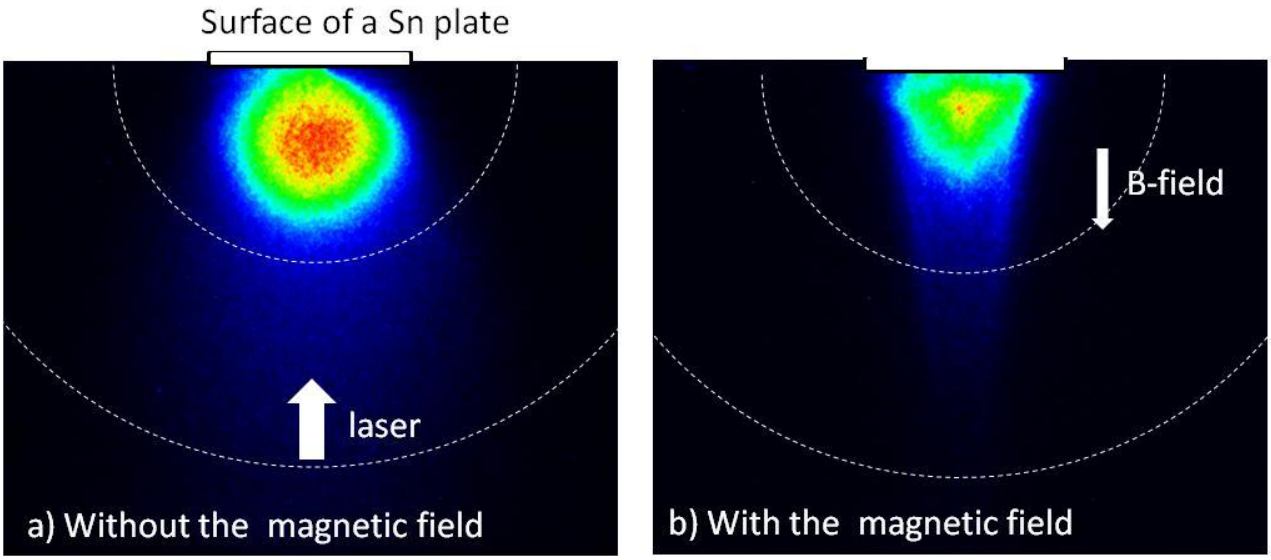


Figure 9. Contour images of the neutral distributions generated from a planar Sn target

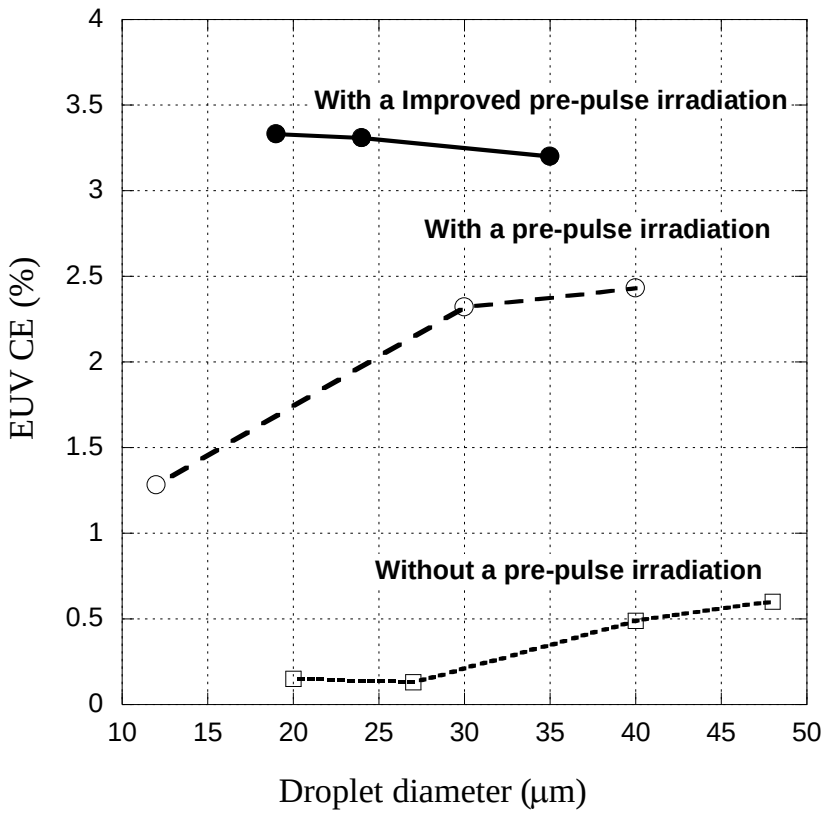


Figure 10. EUV CE as a function of the droplet diameter

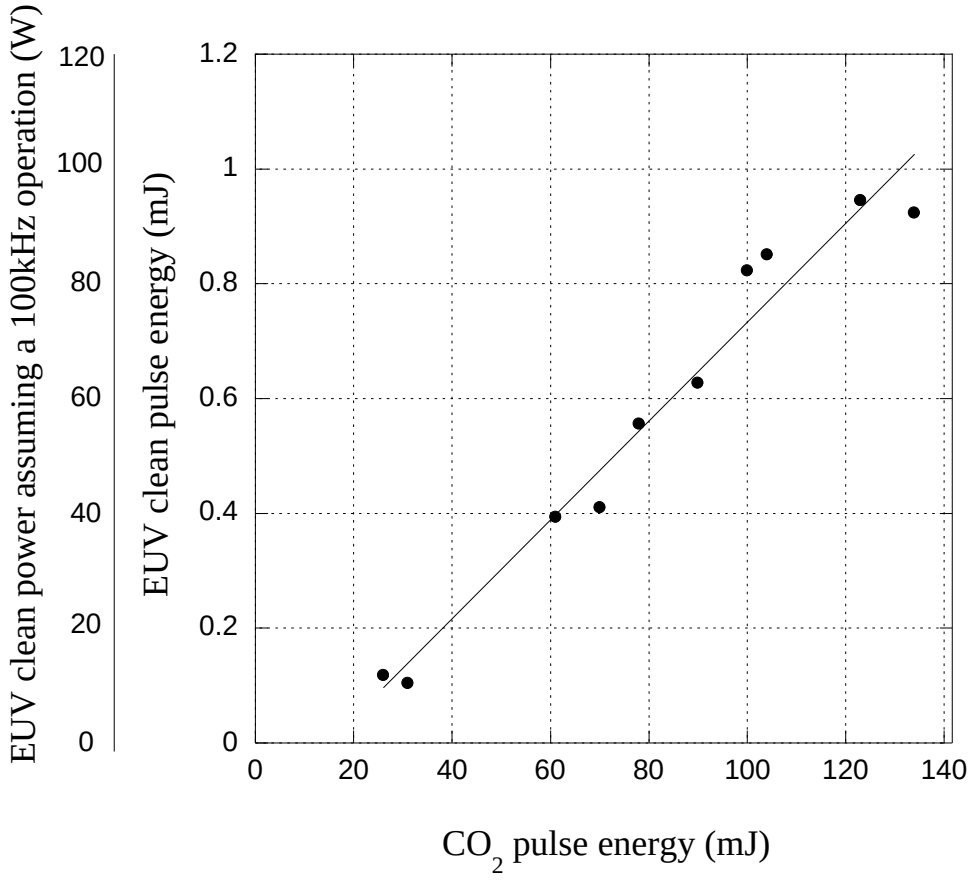


Figure 11. CO2 pulse energy vs., EUV clean pulse energy

## 5. CONCLUSIONS

The optimization of tin debris mitigation with the compact EUV generation system is presented. We confirmed that the Sn fragments generated from the 20 μm diameter droplet after the pre-pulse irradiation was vaporized almost entirely by adjusting the pre-pulse laser and main-pulse laser parameters. The Sn neutral atoms after the pre-pulse laser irradiation were observed with the LIF method. The Sn atoms from the planar target are converged and ejected along the magnetic field. This result proves the magnetic field is beneficial to the Sn particles guiding of not only the ions but also the neutral atoms. Finally the EUV CE with the droplet target is measured. The EUV- CE of 3.4% for the 20 μm diameter droplet is demonstrated by optimizing the pre-pulse laser conditions. We thus obtained the way of the debris reduction with the use of the 20 μm diameter droplet target without the degradation of the EUV CE. These basic studies contribute to the development of the high-power production machine and to the basic design for further EUV power scaling together with theoretical calculations.

## ACKNOWLEDEGEMENT

A part of this work was supported by the New Energy and Industrial Technology Development Organization (NEDO), Japan.

## REFERENCES


[1] Akira Endo, Hideo Hoshino, Takashi Suganuma, Masato Moriya, Tatsuya Ariga, Yoshifumi Ueno, Masaki Nakano, Takeshi Asayama, Tamotsu Abe, Hiroshi Komori, Georg Soumagne, Hakaru Mizoguchi, Akira Sumitani and Koichi Toyoda, Proc. of SPIE Vol.6517, 65170O, (2007).

[2] Yoshifumi Ueno, Hideo Hoshino, Tatsuya Ariga, Taisuke Miura, Masaki Nakano, Hiroshi Komori, Georg Soumagne, Akira Endo, Hakaru Mizoguchi, Akira Sumitani and Koichi Toyoda, Proc. of SPIE Vol.6517, 65173B, (2007).

[3] Yoshifumi Ueno, Georg Soumagne, Masato Moriya, Takashi Suganuma, Tamotsu Abe, Hiroshi Komori, Akira Endo, and Akira Sumitani, Proc. SPIE 6921, 69212Z (2008).

[4] Yoshifumi Ueno, Georg Soumagne, Takashi Suganuma, Takayuki Yabu, Masato Moriya, Hiroshi Komori, Tamotsu Abe, Akira Endo, and Akira Sumitani, Proc. SPIE 7005, 70052U (2008).

[5] Yoshifumi Ueno, Georg Soumagne, Akira Sumitani, Akira Endo, Takeshi Higashiguchi and Noboru Yugami, Appl. Phys. Lett. 92, 211503 (2008).

[6] Hitoshi Nagano, Tamotsu Abe, Shinji Nagai, Masaki Nakano, Yoshihiko Akanuma, Shin Nakajima, Kouji Kakizaki, Akira Sumitani, Junichi Fujimoto, Hakaru Mizoguchi, Proc. SPIE 7636, 76363C (2010).

[7] Yoshifumi Ueno, Tatsuya Yanagida, Takashi Suganuma, Hiroshi Komori, Akira Sumitani, Akira Endo, Proc. SPIE 7361, 73610X(2009).

[8] Shinsuke Fujioka, Masashi Shimomura, Yoshinori Shimada, Shinsuke Maeda, Hirokazu Sakaguchi, Yuki Nakai, Tatsuya Aota, Hiroaki Nishimura, Norimasa Ozaki, Atsushi Sunahara, Katsunobu Nishihara, Noriaki Miyanaga, Yasukazu Izawa and Kunioki Mima, Appl. Phys. Lett. 92, 241502(2008)

[9] D. Nakamura, K. Tamaru, T. Akiyama, A. Takahashi, T. Okada, Appl Phys A 92, 767 (2008)